Supplementing Information

Ratiometric 3D DNA Machine Combined with Machine Learning Algorithm for Ultrasensitive and High-Precision Screening of Early Urinary Diseases

Na Wu[a], Xin-Yu Zhang[b, c], Jie Xia[d], Xin Li[b], Ting Yang[a], Jian-Hua Wang[a]*

[a] Research Center for Analytical Sciences, Department of Chemistry, College of Sciences, Northeastern University, Box 332, Shenyang 110819, China

[b] General Hospital of Northern Theater Command, Shenyang 110015, China

[c] Dalian Medical University, Box 9, Dalian 116044, China

[d] Product Research Institute, Research & Development Center, Huayou Nonferrous Industrial Group, Zhejiang Huayou Cobalt Co. Ltd., Quzhou 324000, China

*Corresponding author: yangting@mail.neu.edu.cn.

Supplementary Experimental Details

Materials. All the oligonucleotides were synthesized and purified by Shanghai Sangon Biotechnology Co. Ltd. (Shanghai, China), and their sequences are listed in Table S1. All oligonucleotide stock solutions were prepared by dissolving DNA strands in Tris-HCl buffer (10 mmol L^{-1} Tris, 10 mmol L^{-1} $MgCl_2$, pH 8.0) and stored at -20 °C refrigerator before use. All the DNA strands were annealed at 95 °C for 5 min and slowly cooled down to room temperature to obtain stable structures. 1-Ethyl-3-[3-(dimethylamino)-propyl] carbodiimide hydrochloride (EDC) and N-hydroxysuccinimide (NHS) were purchased from Aladdin Reagent Co. Ltd. (Shanghai, China). Sodium hydroxide (NaOH), $Na_2HPO_4 \cdot 12H_2O$, $NaH_2PO_4 \cdot 2H_2O$, $AgNO_3$ and KCl were purchased from Sinopharm Chemical Reagent Co. Ltd (Shanghai, China). 2-(N Morpholino) ethanesulfonic acid (MES), Gel-Red, loading buffer and 5×TBE buffer were purchased from Sangon Biotechnology Co. Ltd. (Shanghai, China). BCA Protein Quantification Kit was provided by Beyotime Biotechnology (Shanghai, China). Dulbecco's modified eagle medium (DMEM) was acquired from Aladdin Reagent Co. Ltd. (Shanghai, China). Carboxyl magnetic nanoparticles (COOH-MNPs, 200 nm) was purchased from PuriMag Biotech Co. Ltd. (Xiamen, China). Exo III, phi29 DNA polymerase were purchased from Sangon Biotechnology Co. Ltd. (Shanghai, China). T4 DNA ligase and deoxynucleotides (dNTPs) were purchased from Takara Biotechnology Co. (Dalian, China). Thioflavine T (ThT) was obtained from Yuanye Bio-Technology Co. Ltd. (Shanghai, China). Anti-CD63 rabbit monoclonal antibody(ab193349) was purchased from Abcam Co. Ltd. (Shang, China). Anti-CD9 rabbit monoclonal antibody (20597-1-ap), anti-TSG101 rabbit monoclonal antibody (28283-1-AP) and β-actin monoclonal antibody (66009-1-Ig) were purchased from Proteintech Group Co. Ltd. (Chicago, USA). ELISA (human CD63) kit was purchased from Shanghai Hengyuan Biological Technology (Shanghai, China). All chemicals were analytical grade and directly used without further purification. The solutions were prepared using deionized water (18 MΩ cm^{-1}).

Apparatus. The fluorescence spectra were recorded by a F-7000 fluorescence spectrophotometer (Hitachi High Technologies, Japan). Fluorescence emission spectra

were recorded from 550 to 700 nm at room temperature with a 528 nm-excitation wavelength. The slits for both excitation and emission were set to be 10 nm. The morphologies of uEVs were observed by a transmission electron microscope (TEM) at an accelerating voltage of 200 kV (Tecnai G20, FEI, USA). The image of gel electrophoresis was scanned by the gel imaging analysis system (Shanghai Furi Science & Technology Co., Ltd.). The feasibility of the ratiometric 3D DNA machine was confirmed by a total internal reflection fluorescence microscopy (TIRF, USA). Nanoparticle tracking analysis (NTA) was carried out by NanoSight NS500 (Malvern Instrument, England).

Urine Samples Collection. The normal urine samples (appr. 500 mL per person) were collected from 25 healthy volunteers in the laboratory. (Aged 25-30, 15 males and 10 females with no serious systemic disease, and females are not in menstrual cycle at the time of collection) Urine samples (appr. 500 mL per person) of patients from 13 cases of bladder cancer patients, 13 cases of kidney stones patients and 12 cases of renal cysts patients were collected at the Northern Theater General Hospital. Urine collection was approved by all patients and the ethics committee of General Hospital of Northern Theater Command. Protease inhibitors were added (1.67 mL of 100 mM NaN_3, 2.5 mL of 11.5 mM PMSF, and 50 mL of 1 mM leupeptin for every 50 mL urine) immediately after collection to avoid proteolysis. The urine samples were centrifuged at 2000 g for 20 min at 4 °C to remove whole cells and cell debris. Afterward, urine supernatants were stored at -20 °C until further use.

For the validation of staging diagnostic ability of this approach, urine samples from patients suffering from bladder cancer at different stages were collected from the Liaoning Cancer Hospital and Institute. Briefly, 500 mL of urine sample were collected from each patient in an independent validation cohort (n = 11; that is, 3 for stage I (S1, S2 and S3), 4 for stage II (M1, M2, M3, M4 and M5), 5 for stage III (H1, H2, H3, H4 and H5)). The urine samples were treated in the same procedure as described above. All experiments involving urinary samples are performed in compliance with the relevant laws and institutional guidelines and have been

approved by the ethical committee of Northeastern University, China (No. NEU-EC-2021B008S).

Preparation of uEVs. The uEVs were purified and isolated by multiple steps of ultracentrifugation following previous work.[1] Briefly, the thawed urine sample was subjected to serial centrifugation to remove cells, cellular debris (2000 g for 20 min) and apoptosis body (60000 g for 30 min). As the interfering protein, Tamm-Horsfall Protein (THP) was removed by incubating the resuspended urine supernatant with the reducing agent DTT and ultracentrifuged at 110 000 g for 60 min at 4 °C using a Hitachi Refrigerated Centrifuge (Hitachi, Tokyo, Japan) to sediment the low-density fraction. The low-density sediment was resuspended in 0.01 mol L^{-1} of PBS solution and ultracentrifuged at 110,000 g for 70 min at 4 °C again. Finally, the uEVs were dispersed in PBS buffer (pH=7.4) and stored at -80 °C before further use.

Characterization of uEVs. Traditional characterization of uEVs was performed using NTA, TEM and WB.

NTA Characterization. To quantify the concentration and size distribution of uEVs samples, NTA analysis at 20 ± 3 °C were conducted. Those uEVs concentrations were adjusted to 10^8-10^{10} particles mL^{-1} to obtain counting accuracy. The data of size distribution were captured and analyzed with the ZetaView software.

TEM Characterization. The uEVs suspended in PBS were dropped onto a carbon coated copper grid and allowed to stand for 20 min. The excess solution was absorbed with filter paper. Next, 1.5% phosphotungstic acid was dropped onto the above grid and incubated for 4 min to stain the samples. Subsequently, the grid was dried under the incandescent lamp and observed by TEM at 200 kV.

Western Blotting Analysis. The proteins concentration of samples was measured with BCA protein assays. Subsequently, 5 ×loading buffer was added in the uEVs protein samples separately and the samples were heated at 100 ℃ for 6 min to denature the proteins. Then the proteins were resolved by electrophoresis using SDS-PAGE and transferred onto a polyvinylidene fluoride (PVDF) microporous membrane (Merck Millipore, Immobilon-P Transfer Membrane) through the wet membrane transfer device (Tanon Science & Technology Co., Ltd.). The PVDF membrane was

rinsed and blocked with western blocking agent (Dalian Meilun Biotechnology Co. Ltd.) for 2 h at 37 ℃. Next, the PVDF membrane was incubated with different antibody separately at 4 ℃ overnight. After rinsing, PVDF membrane was incubated with the secondary antibody (anti-rabbit antibody 1:5000; anti-mouse antibody 1:10000) for 2 h at 37 ℃. Lastly, blots were presented through Tanon-4100 Imaging System (Tanon Science & Technology Co. Ltd.).

Electrophoresis Analysis. Nondenaturing polyacrylamide gel electrophoresis (PAGE) was used to confirm the DNA walking process. The concentration of each DNA sample was set as 1 μM. Subsequently, the DNA sample (10 μL) was mixed with loading buffer (2 μL) and added to 15% polyacrylamide gel. The gel was run at constant voltage of 120 V for 40 min in 1×TBE buffer (4.5 mM Tris-HCl, 4.5 mM boric acid, and 0.1 mM EDTA, pH 8.0) followed by staining with 4S Red Plus for 35 min. Gel images were obtained by an UV digital imaging system (Shanghai Furi Science & Technology Co. Ltd.). Agarose gel electrophoresis (1%) was used to investigate the RCA products in 0.5 × TBE buffer at a 90 V constant voltage for 30 min at room temperature.

Statistical Analysis. The difference for protein expression levels from different uEVs were tested using a two-tailed t-test by IBM SPSS Statistics version 19.0 software. The differences were considered to be significant at $p<0.05$. (**$p < 0.01$, ***$p < 0.001$, ****$p < 0.0001$). Each test was performed independently for three times, which were shown as the mean ± standard deviation (SD). Data were visualized using Heml 1.0, Origin version 8.5 software and Python 3.8 with Scikit learn open libraries. A tSNE algorithm was applied for reducing the dimensionality of complex data. tSNE was calculated with EZKit (Version 1.0, EZKit LLC. USA) and the algorithm was based on the research of Laures van der Maaten and Geoffrey Hinton (van der Maaten & Hinton, 2008).[2] Receiver operating characteristic (ROC) curves were used to determine the diagnostic accuracy, which was prepared using MedCalc statistical software. All data derived from each experiment was repeated for three times.

Table S1. Sequences of the oligonucleotides used in this study.

Name	Sequences (5'-3')
Walker-PSA	**TAGC ATTT ACG TGT CAC GCT**
Walker-EpCAM	**TAGC ATTT ACG TGT CAC AGG**
Walker-MUC1	**TAGC ATTT ACG TGT CAC TGT**
Walker-CEA	**TAGC ATTT ACG TGT CAC GGG**
Walker-CD63	**TAGC ATTT ACG TGT CAC TAG**
AS	**AAATTTAAAAAAAAAAAAAAAAAAACCCAAGCTGCTCCTAAATTG TGACACGTAAATGCTA**
AgNCs	**AATTTAGGAGCAGCACCCACCCACCCACCCA**
PLP	**ATCTCGACTAACCCTAACCCTAACCCTAACCCTCAGCTTTTTTTTT TTTTTTTTTTTTGTCTCGGAT**
EpCAM	**CAC TAC AGA GGT TGC GTC TGT CCC ACG TTG TCA TGG GGG GTT GGC CTG TG ACA CGA AAA T GCTA**
MUC1	**AACCGCCCAAATCCCTAAGAGTCGGACTGCAACCTATGCTATCGT TGATGTCTGTCC AAGCAACACAGACACACTACACACGCACAG TG ACA CGA AAA T GCTA**
CEA	**TCG CGC GAG TCG TCT GGG GAA CCA TCG AGT TAC ACC GAC CTT CTA TGT GCG GCC CCC CGC ATCGTC CTC CCG TG ACA CGA AAA T GCTA**
PSA	**AAT TAA AGC TCG CCA TCA AAT AGCG TG ACA CGA AAA T GCTA**
CD63	**CAC CCC ACC TCG CTC CCG TGA CAC TAA TGC TAG TG ACA CGA AAA T GCTA**
Random DNA	**TACGTCTTTCACCTTTCCGCATCGTACTAACGATT**

Table S2. The linear relationship between the fluorescence intensity ratio (F_{ThT}/F_{AgNCs}) and the logarithm of the concentration of uEVs for 5 protein biomarkers from healthy group and three types of urinary disease.

	CD63	PSA	EpCAM	MUC1	CEA
Healthy	F_{ThT}/F_{AgNCs} = 0.863 logc-3.67 (R^2=0.988)	F_{ThT}/F_{AgNCs} = 0.286 logc-1.11 (R^2=0.995)	F_{ThT}/F_{AgNCs} = 0.794 logc-3.58 (R^2=0.984)	F_{ThT}/F_{AgNCs} = 0.267 logc-1.22 (R^2=0.993)	F_{ThT}/F_{AgNCs} = 0.387 logc-1.40 (R^2=0.998)
Bladder	F_{ThT}/F_{AgNCs} = 1.825 logc-7.77 (R^2=0.988)	F_{ThT}/F_{AgNCs} = 1.078 logc-4.41 (R^2=0.992)	F_{ThT}/F_{AgNCs} = 1.188 logc-4.95 (R^2=0.998)	F_{ThT}/F_{AgNCs} = 0.390 logc-1.74 (R^2=0.989)	F_{ThT}/F_{AgNCs} = 1.792 logc-7.58 (R^2=0.978)
Kidney stone	F_{ThT}/F_{AgNCs} = 1.722 logc-7.95 (R^2=0.993)	F_{ThT}/F_{AgNCs} = 0.878 logc-3.79 (R^2=0.998)	F_{ThT}/F_{AgNCs} = 1.007 logc-4.46 (R^2=0.997)	F_{ThT}/F_{AgNCs} = 0.396 logc-1.69 (R^2=0.957)	F_{ThT}/F_{AgNCs} = 1.091 logc-4.68 (R^2=0.997)
Renal cyst	F_{ThT}/F_{AgNCs} = 0.883 logc-4.03 (R^2=0.985)	F_{ThT}/F_{AgNCs} = 0.499 logc-2.04 (R^2=0.998)	F_{ThT}/F_{AgNCs} = 0.523 logc-2.35 (R^2=0.993)	F_{ThT}/F_{AgNCs} = 0.739 logc-3.29 (R^2=0.989)	F_{ThT}/F_{AgNCs} = 0.916logc-4.11 (R^2=0.998)

Table S3. Comparison of the analytical performance of the present method with some common DNA machine approaches for uEVs detection.

Method	LOD (particles/mL)	DNA machine	Detection range (particles/mL)	ref
Fluorescence	8.2×10^{3}	DNA walker	2.4×10^{4}-2.0×10^{9}	3
Electrochemical	7×10^{4}	Exo III-assisted DNA recycling	10^{6}-10^{8}	4
Electrochemical	1.2×10^{4}	Aptamer Recognition-Induced Multi-DNA Release +ERA	3.4×10^{4}-3.4×10^{8}	5
Electrochemiluminescence	6×10^{4}	DNA walker	2×10^{5}-7.5×10^{7}	6
Fluorescence	1×10^{5}	RCA+ nicking endonuclease (Nb·BbvCI) assisted target recycling	10^{6}-10^{8}	7
Electrochemical	1.3×10^{4}	DNA walker +ERA	5×10^{4}-10^{10}	8
Fluorescence	9.9×10^{3}	DNA walker +RCA	10^{4}-10^{8}	This work

Table S4. Summary of the bladder cancer stage cohort.

Stage I			Stage II			Stage III		
No	**Sex**	**TNM**	**No**	**Sex**	**TNM**	**No**	**Sex**	**TNM**
S1	**Female**	**T1N0M0**	**M1**	**Male**	**T1N0M0**	**H1**	**Male**	**T3N0M0**
S2	**Male**	**TaN0M0**	**M2**	**Male**	**T1N0M0**	**H2**	**Male**	**T3N0M0**
S3	**Male**	**TaN0M0**	**M3**	**Female**	**T3N2M0**	**H3**	**Male**	**T3N0M0**
			M4	**Female**	**T3N2M0**	**H4**	**Female**	**T4N0M0**
						H5	**Female**	**T4N0M0**

Table S5. Summary of the heatmap cohort.

Characteristic	Male	Female
Healthy (n=10)	3	7
Bladder cancer (n=10）	6	4
Kidney stone (n=10)	5	5
Renal cyst (n=10)	6	4
Total disease (n=30)	17	13

Table S6. Summary of the algorithms training cohort.

Characteristic	Male	Female
Healthy (n=25)	**10**	**15**
Bladder cancer (n=13）	**7**	**6**
Kidney stone (n=13)	**9**	**4**
Renal cyst (n=11)	**8**	**3**
Total disease (n=63)	**24**	**13**

Table S7. Performance of uEVs biomarkers to differentiate urinary diseases and healthy control in the ROC cohort.

Biomarker	AUC	Biomarker	AUC
CD63	0.821	CD63+PSA+MUC1	0.745
PSA	0.740	CD63+PSA+CEA	0.834
EpCAM	0.769	PSA+EpCAM+MUCA	0.728
MUC1	0.622	PSA+EpCAM+CEA	0.844
CEA	0.783	EpCAM+MUC1+CEA	0.822
CD63+CEA	0.888	CD63+EpCAM+MUC1	0.767
CD63+EpCAM	0.852	CD63+EpCAM+CEA	0.916
CD63+PSA	0.787	CD63+PSA+EpCAM+CEA	0.931
CD63+MUC1	0.679	CD63+PSA+MUC1+CEA	0.835
EpCAM+CEA	0.858	CD63+PSA+EpCAM+MUC1	0.819
EpCAM+MUC1	0.634	CD63+EpCAM+MUC1+CEA	0.878
MUC1+CEA	0.679	PSA+EpCAM+MUC1+CEA	0.804
CD63+PSA+EpCAM	0.815	CD63+PSA+EpCAM+MUC1+CEA	0.973

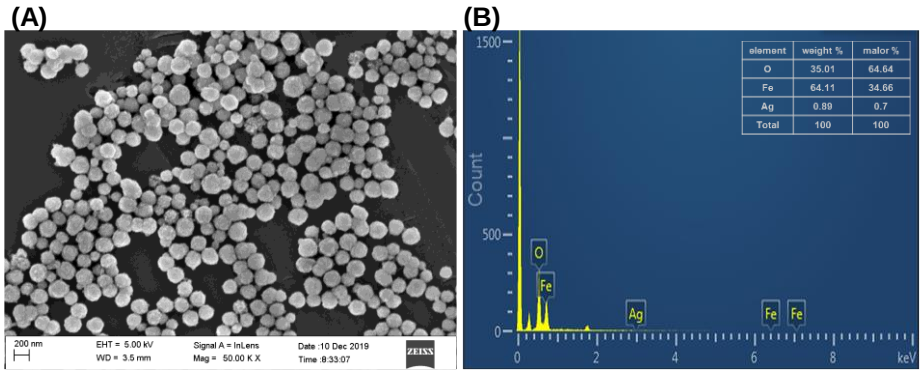

Figure S1. (A) SEM image of MNPs. (B) EDS Spectrum of AgNCs-MNPs. Scale bar represents 200 nm.

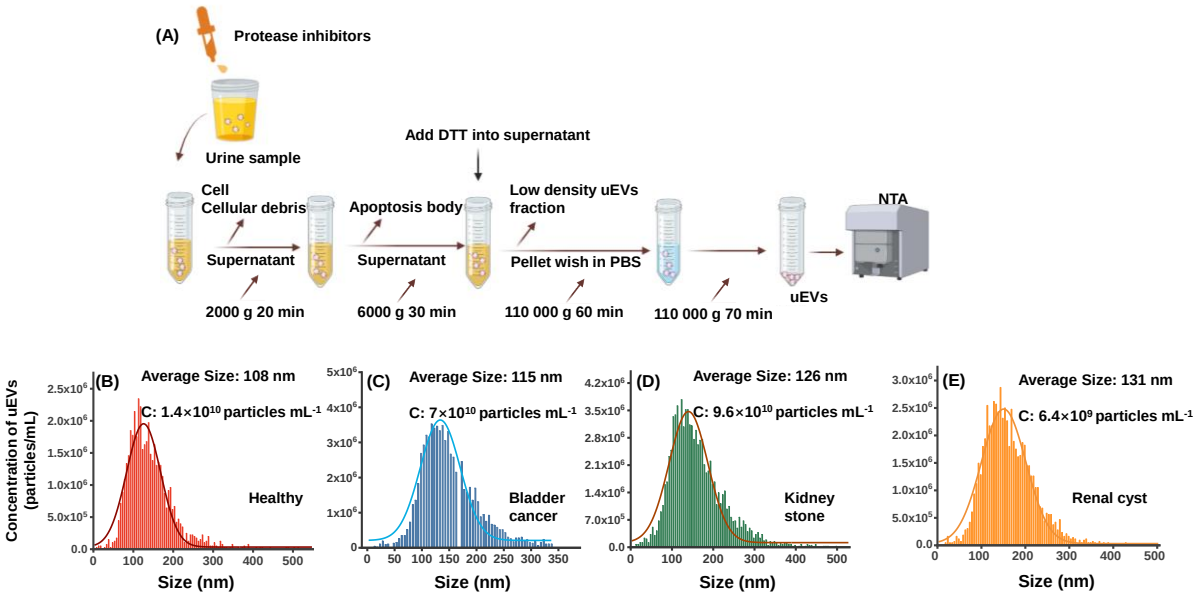

Figure S2. Evaluation of the isolated uEV. (A) The uEV isolation procedure by ultracentrifugation separation. Size distribution and concentration of uEVs derived from (B) healthy donors, (C) bladder cancer, (D) kidney stone, and (E) renal cyst. Data were obtained by NTA analysis and are represented as the means ± SDs (n = 3). (C = concentration). Figure S2A is created by BioRender apps. with authorized license.

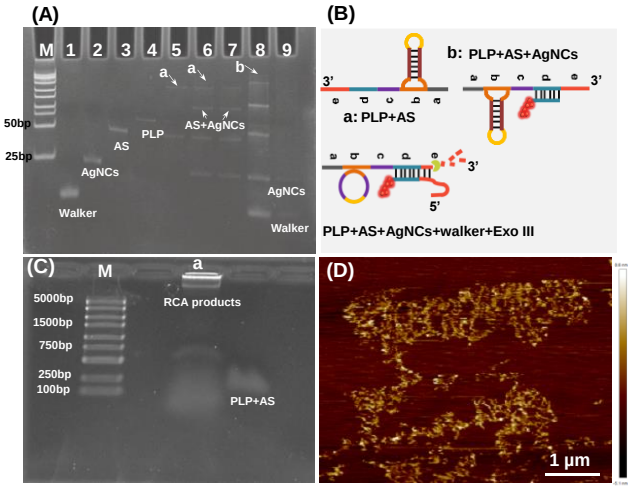

Figure S3. (A) Native PAGE characterization of the DNA walkers process (Lane 1: Walker; Lane 2: AgNCs; Lane 3:AS; Lane 4: PLP, Lane 5: PLP+AS, Lane 6: PLP+AgNCs+AS, Lane 7: PLP+AgNCs+AS+Exo III; Lane 8: PLP+AgNCs+AS+Walker; Lane 9: PLP+AgNCs+AS+Walker+Exo III; (B) Schematic of DNA complementary pairing involved in the DNA walkers process; (C) Agarose gel (1%) electrophoresis for the characterization of the RCA process. lane M: DNA marker; Lane a: RCA products. (D) AFM image of RCA product. Scale bar represents 5 μm.

The PAGE analysis was applied to verify the 3D DNA walkers process and the AGE analysis was used to confirm the RCA product. As shown in Figure S3A, the bands in lanes 1, 2, 3 and 4 correspond to walker, $DNA_{(AgNCs)}$ (labeled as AgNCs for short), AS and PLP, respectively. In lane 5, the appearance of a new upper band compared to those band in lane 3 (AS) and lane 4 (PLP) demonstrates the efficient hybridization between AS and PLP. In lane 6, the AS/PLP/ AgNCs complexes was not observed, which may because of a too low concentration. In the presence of Exo III (lane 7), the AS/PLP/ AgNCs complex cannot be digested by Exo III thus was clearly indicated. The reason is that the AS/PLP/ AgNCs complex form a recessed 3′-end. It is shown in lane 8 that the mixture of walker, AS, PLP and AgNCs results in a brighter band. When Exo III was added into the mixture of the four strands (lane 9), the hybridization bands disappear while walker and AgNCs strands appear. The PAGE results confirmed that the walkers process could be proceeded in the presence of Exo III and target as the proposed walking mechanism. Furthermore, the digestion products trigger the RCA process and then produces large number of G-rich sequences. Further support of the RCA products was also obtained by AEG and AFM. In the AEG image (Figure S3C), a strong band corresponding to chains in excess of

the maximum marker length of 5000 bp per chain was observed, which would lead to chains of DNA several micrometers in length. After drop-casting a dilute solution of this DNA onto a freshly cleaved mica surface, we observed long, coiled DNA chains micrometers in length (Figure S3D). The AFM image result was consistent with the AEG analysis.

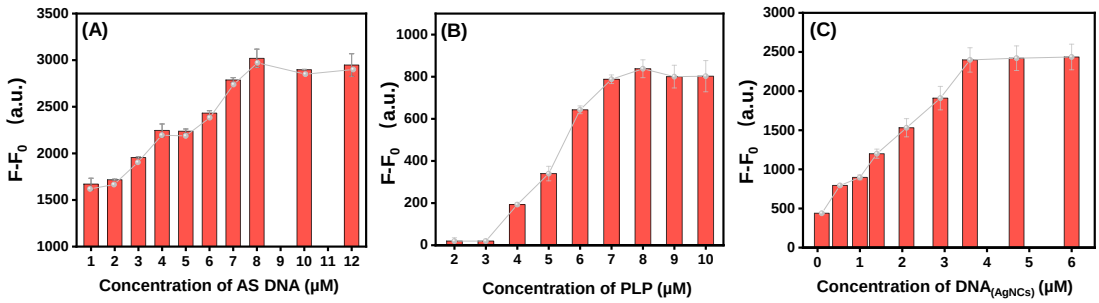

Figure S4. The effect of various parameters on the pre-assemble of ratiometric 3D DNA machine. (A) Concentration of AS DNA; (B) Concentration of PLP; (C) Concentration of $DNA_{(AgNCs)}$. uEVs concentration: 1×10^5 particles mL^{-1}. Error bar represents ± SD (n = 3)

Optimization of the Experimental Conditions. Some of the key experimental conditions were thoroughly investigated for optimizing the performance of the ratiometric 3D DNA machine. The assembly efficiency of AS, $DNA_{(AgNCs)}$, and PLP on MNPs surface would affect the performance of ratiometric 3D DNA machine; The concentration of AS DNA of this preassembled ratiometric 3D DNA machine was investigated by fixing the following parameters and monitoring the signal at different concentration gradient. The FAM and NH_2 co-labeled AS (100 μL) were mixed with 1 mL of the EDC/NHS- activated MNPs (10 mg mL^{-1}) solution and incubated overnight at 25 °C. Afterwards, the FAM-AS-conjugated MNPs were magnetically separated, washed for three times and re-suspended for the monitoring of fluorescent intensity at 517 nm (emitted by FAM). As shown in Figure S4A, the fluorescent intensity increases as the AS concentration increases, and 8 μM (the concentration we finally chose) of NH_2-teminated AS is enough to get saturated fluorescent signal.

The optimization of PLP concentration was evaluated by the fluorescent intensity of ThT. For reaction process, 5 μL of PLP (2-10 μM), 5 μL of 10×T4 buffer, T4 DNA ligase, 10 μL of BSA (2 mg mL^{-1}) were mixed with 500 μL of AS-MNPs solution and incubated at 16 °C for 3 h. Subsequently, the above mixture was further mixed with 10 μL of phi29 DNA polymerase (70 U/μL), 10 μL of 10× phi29 DNA polymerase buffer, 3 μL of dNTP (10 mM) and 10 μL of BSA (2 mg mL^{-1}). The reaction mixture was incubated at 37 °C for 1.5 h and denatured at 65 °C for 15 min. The final product (100 μL) was mixed with 6 μM of ThT (50 μL), 10 mM of K^+ (50 μL) and 300 μL of TE buffer (40 mM Tris-HCl, pH 7.5, 50 mM KCl, 10 mM $MgCl_2$). The ultimate

reaction products were subjected to the fluorescence measurement. All fluorescence spectra were measured using a quartz cuvette on a Hitachi F-7000 fluorescence spectrophotometer (Tokyo, Japan). The excitation wavelength was 440 nm, and the emission spectra were recorded over the wavelength from 450 nm to 500 nm with a slit width of 10 nm for both excitation and emission. As shown in Figure S4B, the largest fluorescent intensity of ThT was observed at 8 μM, which was selected as the optimized concentration of PLP.

The optimization of $DNA_{(AgNCs)}$ concentration was evaluated by the fluorescent intensity of AgNCs. For reaction process, 100 μL of $DNA_{(AgNCs)}$ with different concentrations (ranging from 0.5-6 μM) was mixed with 20 μL of $AgNO_3$ (600 μM) and incubated in ice water for 30 min. Then 20 μL of freshly prepared $NaBH_4$ (600 μM) was added into the above mixture with vigorous shaking for 40 s and then incubated at 4 °C in the dark for 5 h. Then, 500 μL of AS-PLP-MNPs complex was added for incubation at 37 °C for 12 h. The resulting AgNCs-MNPs were magnetically separated, washed and re-suspended for the monitoring of fluorescent intensity at 642 nm (emitted by AgNCs). As shown in Figure S4C, the highest fluorescent intensity of AgNCs was observed at 3.6 μM, which was selected as the optimized concentration of $DNA_{(AgNCs)}$.

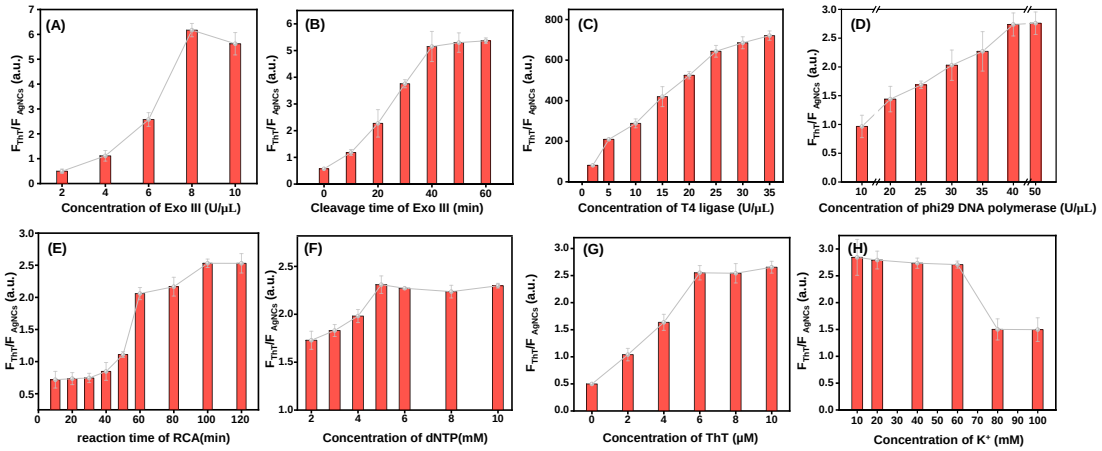

Figure S5. The effect of various parameters on the performance of the ratiometric 3D DNA machine. (A) Concentration of Exo III; (B) Cleavage time of Exo III; (C) Concentration of T4 ligase; (D) Concentration of phi29 DNA polymerase; (E) Reaction time of RCA; (F) Concentration of dNTP; (G) Concentration of ThT; (H) Concentration of K^+; uEVs concentration: 1×10^5 particles mL^{-1}. Error bar represents ± SD (n = 3)

To improve the amplification efficiency of the ratiometric 3D DNA machine, some critical parameters such as the concentration of Exo III, the cleavage time of Exo III, the concentration of T4 ligase and phi29 DNA polymerase, the reaction time of RCA, the concentration of dNTP, ThT and K^+ were optimized. The ratio of F_{ThT}/F_{AgNCs} is used for assessing the assay performance, where F_{ThT} is the fluorescence intensity of ThT, and F_{AgNCs} is the fluorescence intensity of AgNCs. After optimization, the suitable amount of Exo III was set as 8 U/μL with a cleavage time of 40 min. The optimal concentration of T4 ligase and phi29 DNA polymerase was 35 U/μL and 40 U/μL, respectively. The RCA reaction time was optimized as 100 min and the concentration of ThT and K^+ was 6 μM and 10 mM, respectively.

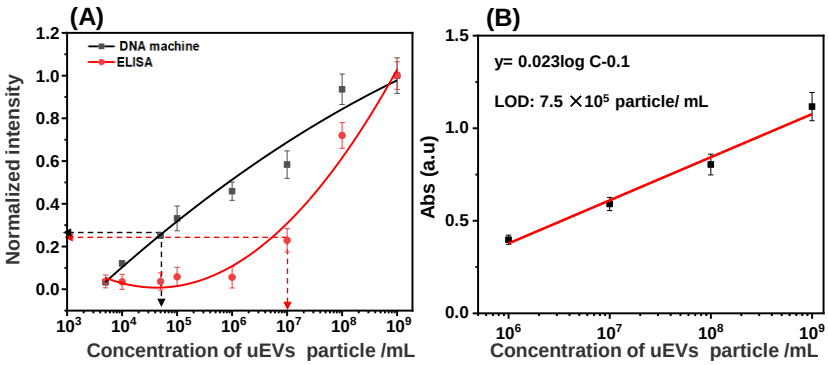

Figure S6. (A) The sensitivity comparison between ratiometric 3D DNA machine and commercial ELISA kit with CD63 as biomarker. (B) Linear relationship between the absorbance and the logarithm of the number of uEV of the commercial ELISA kit for the quantification of surface CD63 of uEV.

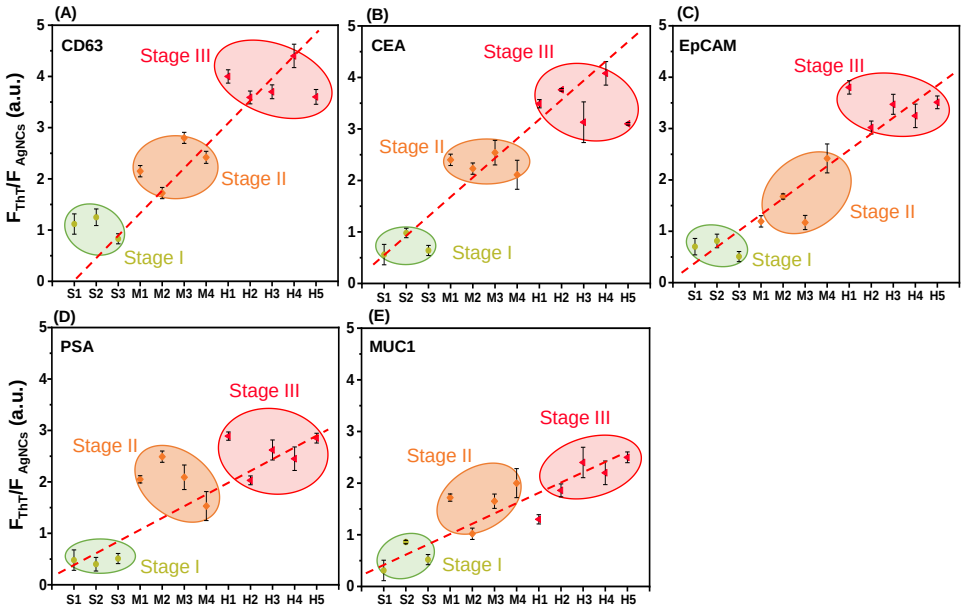

Figure S7. The uEV biomarkers profiles in an independent validation cohort of bladder cancer at different stages (n = 11; that is, 3 for stage I (S1, S2 and S3), 4 for stage II (M1, M2, M3 and M4), 5 for stage III (H1, H2, H3, H4 and H5)) (n = 3 uEV samples, mean ± s.d.)

As can be seen in Figure S7, stage-dependent fluorescence response was observed, in which the fluorescence intensity ratio (F_{ThT}/F_{AgNCs}) gradually increases with the increasing stage. This result suggested the capability of the ratiometric 3D DNA machine to detect and classify urinary diseases at different stage.

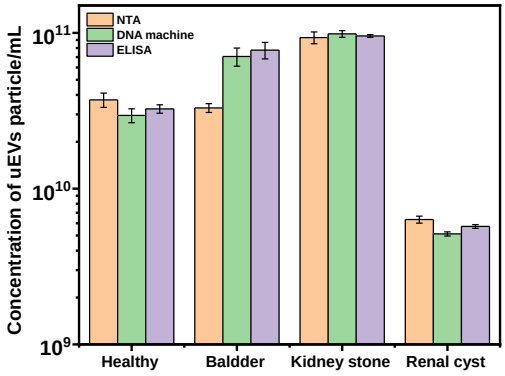

Figure S8. Quantification of uEVs from healthy control and three types of urinary diseases (bladder cancer, kidney stone and renal cyst) by NTA, DNA machine and ELISA. Error bar represents ± SD (n = 3).

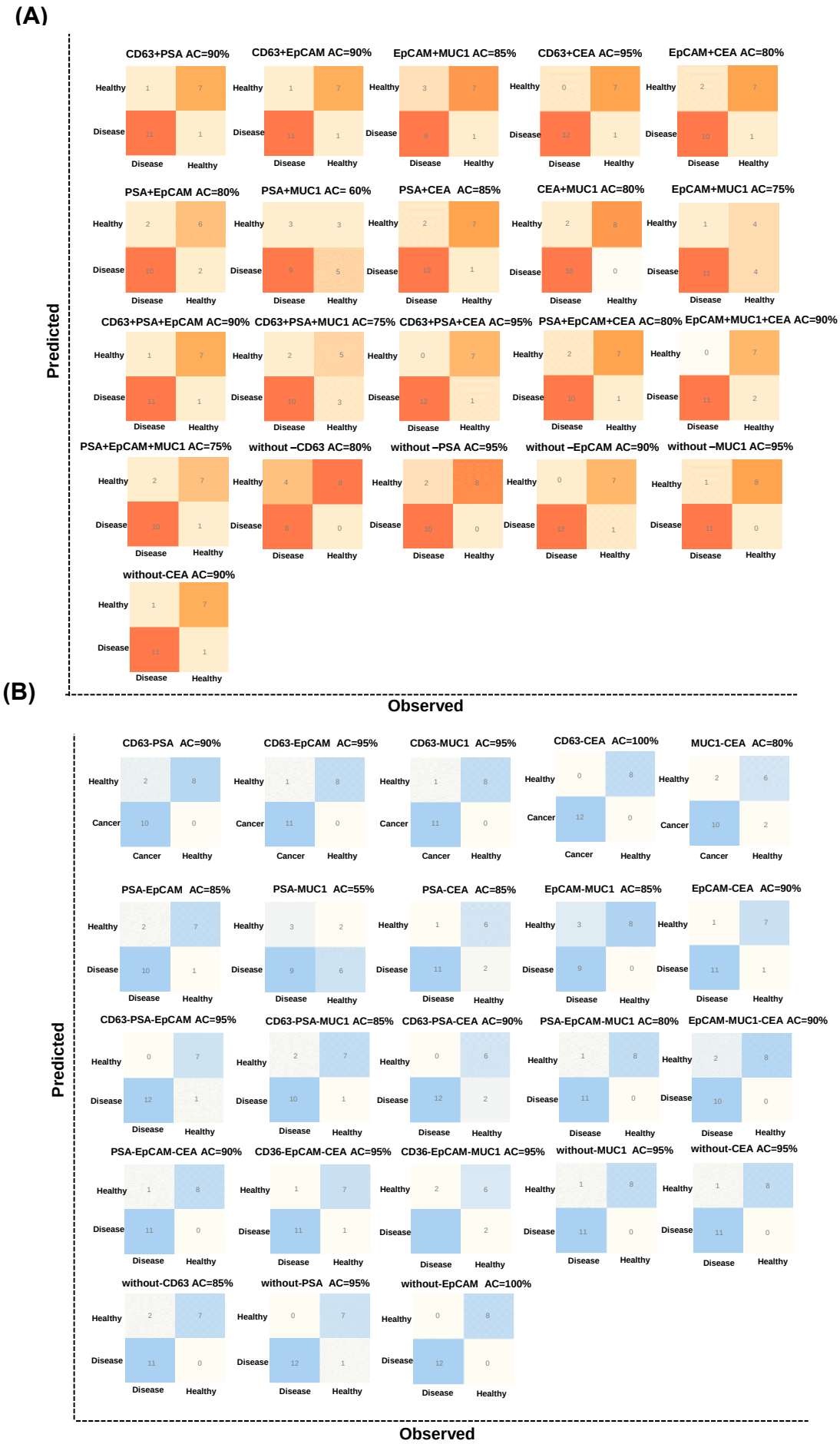
(A)
CD63+PSA AC=90%
CD63+EpCAM AC=90%
EpCAM+MUC1 AC=85%
CD63+CEA AC=95%
EpCAM+CEA AC=80%
PSA+EpCAM AC=80%
PSA+MUC1 AC= 60%
PSA+CEA AC=85%
CEA+MUC1 AC=80%
EpCAM+MUC1 AC=75%
CD63+PSA+EpCAM AC=90%
CD63+PSA+MUC1 AC=75%
CD63+PSA+CEA AC=95%
PSA+EpCAM+CEA AC=80%
EpCAM+MUC1+CEA AC=90%
PSA+EpCAM+MUC1 AC=75%
without –CD63 AC=80%
without –PSA AC=95%
without –EpCAM AC=90%
without –MUC1 AC=95%
without-CEA AC=90%
Predicted
Observed
Healthy
Disease
(B)
CD63-PSA AC=90%
CD63-EpCAM AC=95%
CD63-MUC1 AC=95%
CD63-CEA AC=100%
MUC1-CEA AC=80%
PSA-EpCAM AC=85%
PSA-MUC1 AC=55%
PSA-CEA AC=85%
EpCAM-MUC1 AC=85%
EpCAM-CEA AC=90%
CD63-PSA-EpCAM AC=95%
CD63-PSA-MUC1 AC=85%
CD63-PSA-CEA AC=90%
PSA-EpCAM-MUC1 AC=80%
EpCAM-MUC1-CEA AC=90%
PSA-EpCAM-CEA AC=90%
CD36-EpCAM-CEA AC=95%
CD36-EpCAM-MUC1 AC=95%
without-MUC1 AC=95%
without-CEA AC=95%
without-CD63 AC=85%
without-PSA AC=95%
without-EpCAM AC=100%
Predicted
Observed
Cancer
Healthy

(C)

	CD63+EpCAM	CD63+PSA+CEA	CD63+EpCAM+CEA+PSA	CD63+EpCAM+CEA+PSA+MUC1
SVM	95%	90%	95%	90%
KNN	78.9%	84.2%	95%	85%
	CD63+PSA	CD63+PSA+EpCAM	CD63+EpCAM+MUC1+CEA	
SVM	90%	95%	95%	
KNN	90%	90%	95%	
	CD63+MUC1	CD63+PSA+MUC1	CD63+EpCAM+MUC1+PSA	
SVM	95%	85%	95%	
KNN	85%	75%	90%	
	CD63+CEA	CD63+PSA+CEA	CD63+MUC1+PSA+CEA	
SVM	100	90%	100%	
KNN	95%	95%	90%	
	EpCAM+PSA	PSA+EpCAM+MUC1	MUC1+EpCAM+PSA+CEA	
SVM	85%	80%	85%	
KNN	80%	90%	80%	
	EpCAM+MUC1	PSA+EpCAM+CEA		
SVM	85%	90%		
KNN	75%	80%		
	EpCAM+CEA	EpCAM+MUC1+CEA		
SVM	90%	90%		
KNN	90%	90%		
	PSA+MUC1			
SVM	55%			
KNN	60%			
	PSA+CEA			
SVM	85%			
KNN	85%			
	MUC1+CEA			
SVM	80%			
KNN	80%			

Figure S9. Optimization of biomarker combination for the training cohort. The performances of all SVMs and KNNs, using 5 markers as the input for binary classification (healthy and disease). Accuracy comparison with SVM and KNN algorithms using different biomarker combinations. Accuracies are defined as the proportion of all individuals that are correctly classified. (A) Accuracy predicted by the KNN in the test set at the patient level. (B) Accuracy predicted by the SVM in the test set at the patient level. (C) KNN and SVM summarized the accuracy of all binary classification combination prediction models. Those models were verified using split data of the training set of 70% and test set of 30%. (Test condition: 5-fold cross validation (CV)

(A)


PSA+CEA AC=73.7%
EpCAM+MUC1 AC=57.9%
EpCAM + CEA AC=68%%
MUC1+ CEA AC=52.6%
CD63+MUC1 AC=52.6%
CD63+EpCAM AC=68.4%
CD63+PSA AC=78.9%
PSA+MUC1 AC=21%
CD63+CEA AC=78.9%
PSA+EpCAM AC=63.2%
CD63+EpCAM+CEA AC=78.9%
EpCAM+MUC1+CEA AC=63.2%
CD63+MUC1+CEA AC=73.7 %
PSA+MUC1+CEA AC=68.4%
PSA+EpCAM+MUC1 AC=57.9%
CD63+EpCAM+MUC1 AC=73.7%
CD63+PSA+EpCAM AC=68.4%
PSA+EpCAM+CEA AC=63.2%
CD63+PSA+CEA AC=73.7%
CD63+PSA+MUC1 AC=52.6%
CD63+PSA+EpCAM+ CEA AC=84.2%
PSA+EpCAM+MUC1+ CEA AC=68.4%
CD63+EpCAM+MUC1+ CEA AC=78.9%
CD63+PSA+MUC1+ CEA AC=73.7%
CD63+PSA+EpCAM+ MUC1 AC=63.2%
CD63+PSA+EpCAM +MUC1+CEA AC=82%
Kidney stone
Healthy
Renal cyst
Bladder
Predicted
Observed

(B)

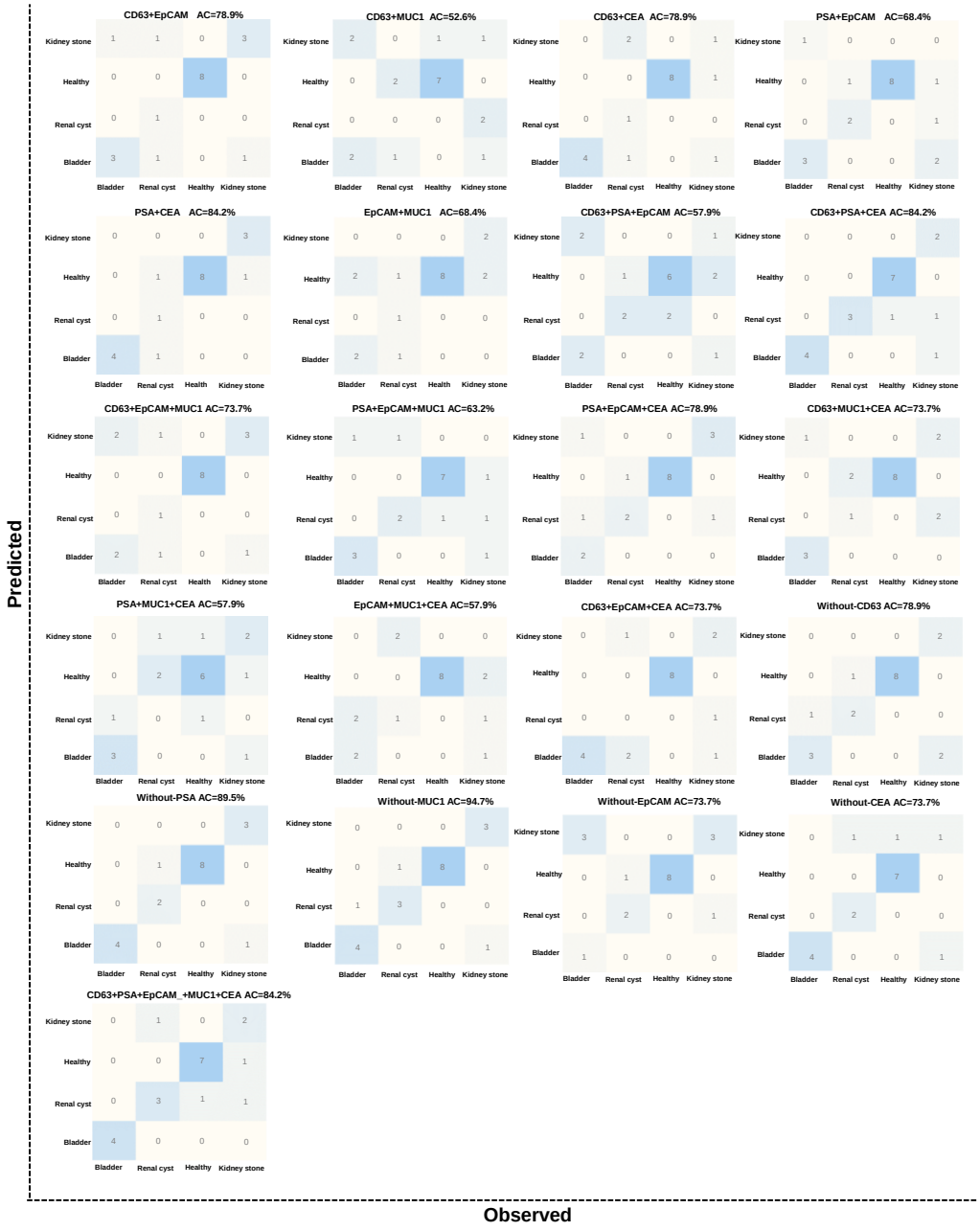
CD63+EpCAM AC=78.9%
CD63+MUC1 AC=52.6%
CD63+CEA AC=78.9%
PSA+EpCAM AC=68.4%
PSA+CEA AC=84.2%
EpCAM+MUC1 AC=68.4%
CD63+PSA+EpCAM AC=57.9%
CD63+PSA+CEA AC=84.2%
CD63+EpCAM+MUC1 AC=73.7%
PSA+EpCAM+MUC1 AC=63.2%
PSA+EpCAM+CEA AC=78.9%
CD63+MUC1+CEA AC=73.7%
PSA+MUC1+CEA AC=57.9%
EpCAM+MUC1+CEA AC=57.9%
CD63+EpCAM+CEA AC=73.7%
Without-CD63 AC=78.9%
Without-PSA AC=89.5%
Without-MUC1 AC=94.7%
Without-EpCAM AC=73.7%
Without-CEA AC=73.7%
CD63+PSA+EpCAM_+MUC1+CEA AC=84.2%
Kidney stone
Healthy
Renal cyst
Bladder
Predicted
Observed

(C)

	CD63+EpCAM	CD63+PSA+CEA	CD63+EpCAM+CEA+PSA	CD63+EpCAM+CEA+PSA+MUC1
SVM	78.9%	84.2%	94.7%	84.2%
KNN	68.4%	73.7%	84.2%	82%
	CD63+PSA	CD63+PSA+EpCAM	CD63+EpCAM+MUC1+CEA	
SVM	×	57.9%	89.5%	
KNN	78.9%	68.4%	78.9%	
	CD63+MUC1	CD63+PSA+MUC1	CD63+EpCAM+MUC1+PSA	
SVM	52.6%	57.9%	73.7%	
KNN	52.6%	52.6%	63.2%	
	CD63+CEA	CD63+PSA+CEA	CD63+MUC1+PSA+CEA	
SVM	78.9%	84.2%	73.7%	
KNN	78.9%	73.7%	73.7%	
	EpCAM+PSA	PSA+EpCAM+MUC1	MUC1+EpCAM+PSA+CEA	
SVM	68.4%	63.2%	78.9%	
KNN	63.2%	52.6%	68.4%	
	EpCAM+MUC1	PSA+EpCAM+CEA		
SVM	68.4%	78.9%		
KNN	57.9%	63.2%		
	EpCAM+CEA	EpCAM+MUC1+CEA		
SVM	63.2%	57.9%		
KNN	68%	63.2%		
	PSA+MUC1	CD63+EpCAM+CEA		
SVM	57.9%	73.7%		
KNN	21.0%	78.9%		
	PSA+CEA			
SVM	84.2%			
KNN	73.7%			
	MUC1+CEA			
SVM	52.6%			
KNN	52.6%			

	Double biomarkers (A-AC)	Three biomarkers (A-AC)	Four biomarkers (A-AC)	Five biomarkers (A-AC)
SVM	60.5%	69.7%	82.1%	84.2%
KNN	61.5%	65.8%	73.7%	82%

Total average accuracy of SVM and KNN were 69.1% and 66.3%, respectively. (Average accuracy: A-AC)

Figure S10. Optimization of biomarker combination for the training cohort. The performances of all SVMs and KNNs, using 5 markers as the input for multi-type urinary diseases (three kinds of

urinary disease and healthy donors). Accuracy comparison with SVM and KNN algorithms using different biomarker combinations. Accuracies are defined as the proportion of all individuals that are correctly classified. (A) Accuracy predicted by the KNN in the test set at the patient level. (B) Accuracy predicted by the SVM in the test set at the patient level. (C) KNN and SVM summarized the accuracy of all multi-types urinary diseases combination prediction models. Those models were verified using split data of the training set of 70% and test set of 30%. Test condition: 5-fold cross validation (CV)

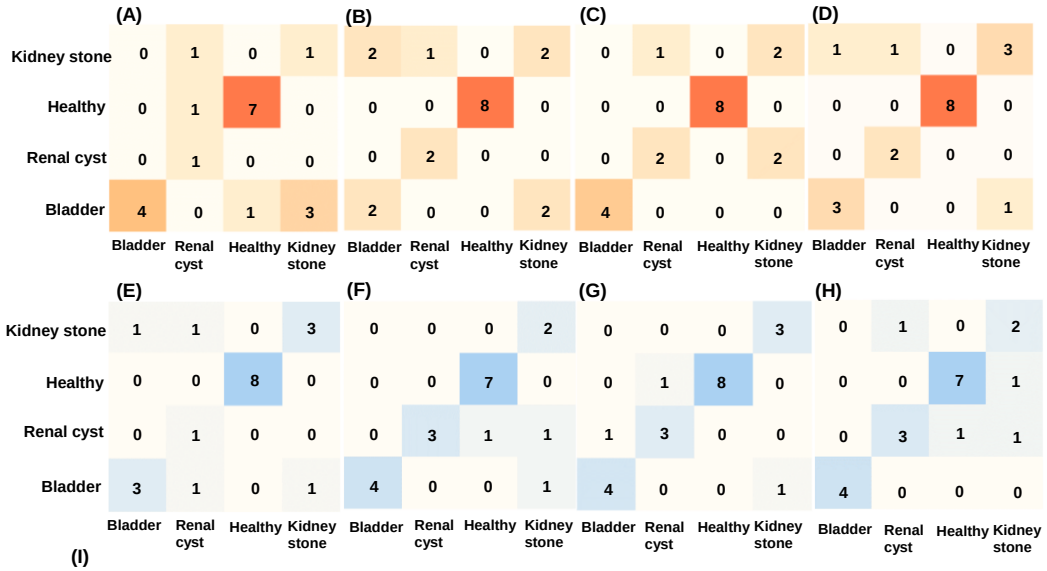

(I)

biomarker / algorithm	CD63+EpCAM (A, E)	CD63+PSA+CEA (B, F)	CD63+EpCAM+CEA+PSA (C, G)	CD63+EpCAM+CEA+PSA+MUC1 (D,H)
SVM	AC=68.4%	AC=73.7%	AC=94.7%	AC=86.1%
KNN	AC=78.9%	AC=84.2%	AC=84.2%	AC=84.2%

Figure S11. Confusion matrix of KNN (A-D) and SVM (E-H) algorithms for diagnosis output the best different biomarker combinations. KNN: (A) CD63+EpCAM, (B) CD63+PSA+CEA, (C) CD63+EpCAM+CEA+PSA, (D) CD63+EpCAM+CEA+PSA+CEA; SVM: (E) CD63+EpCAM, (F) CD63+PSA+CEA, (G) CD63+EpCAM+CEA+PSA, (H) CD63+EpCAM+CEA+PSA+CEA. Bladder cancer: n = 13, kidney stone: n = 13, renal cyst: n=11, and healthy controls (n = 25). The accuracy (AC), which represents the diagnostic performance, was uesd as major parameter. (I) Sammary of AU value of KNN (A-D) and SVM (E-H) algorithms for diagnosis output the best different biomarker combinations.

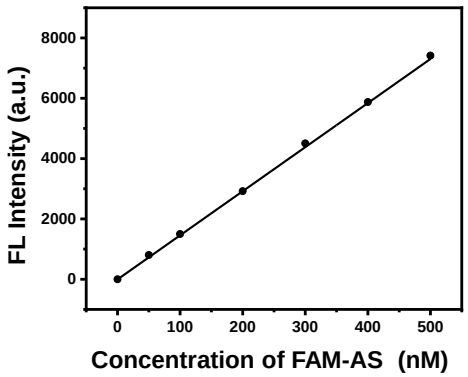

Figure S12. Calibration curve of FAM-conjugated anchor strand (FAM-AS).

The fluorescence was converted to molar concentrations of FAM (5-carboxy fluorescein) by using a calibration curve that was prepared with known concentrations of FAM-anchor strand (Figure S12). The fluorescence intensity of FAM was collected between 500 and 600 nm with the maximum excitation wavelength at 488 nm. FAM-AS-NH_2 ($C_{initial}$: 8 μM, 100 μL) was modified on the surface of MNPs, and followed by magnetic separation. The supernatant fluorescence intensity was then measured.

$FL_{(FAM\text{-}AS\text{-}NH_2 \text{ on the MNPs})} = FL_{control} - FL_{supernatant} = 15780 - 7669 = 8111$

Standard curve linear equation: y=14.6x-5.8

The final concentration of FAM-AS-NH_2 on the MNPs= 555.9 nM

The amount of the AS decorated on MNPs is 555.9×10^{-9} M$\times 600 \times 10^{-6}$ L$= 3.3 \times 10^{-10}$ mol

Note: control group-(AS: $C_{initial}$ 8 μM, 600 μL, Tris-HCl buffer) measurement conditions: slit-10 nm, voltage -700V.

In a typical coupling process, 100 μL of COOH-MNPs (10 mg·mL^{-1}, 600 μM carboxylic acid/g beads) was washed and diluted to 500 μL to react with 100 μL of NH_2-teminated AS (8 μM). The final volume of the reaction system is 600 μL and the total amount of -COOH on MNPs is (600×10^{-6} mol/g beads$\times 600 \times 10^{-3}$ mL$\times 10 \times 10^{-3}$ g·$mL^{-1}$$= 3.6 \times 10^{-6}$ mol), whereas the total amount of added NH_2-AS is (8×10^{-6} M$\times 100 \times 10^{-6}$ L $= 8 \times 10^{-10}$ mol). That is, COOH is excessive compare to NH_2-AS. By measuring the amount of the FAM labeled NH_2-AS before and after coupling reaction, the amount of the AS decorated on MNPs is 3.3×10^{-10} mol. According to the

total amount of -COOH and the amount of AS decorated on the MNPs surface, we can obtain the coupling efficiency to be [(3.3×10^{-10}) / (8×10^{-10})] ×100% =41.25 %.

References

(1) Raj, DAA.; Fiume, I.; Capasso, G.; Pocsfalvi, G. A Multiplex Quantitative Proteomics Strategy for Protein Biomarker Studies in Urinary Exosomes. *Kidney Int.* **2012**, *81*, 1263-1272.

(2) Zhang, J. L.; Shi, J. J.; Zhang, H. L.; Zhu, Y. F.; Liu, W.; Zhang, K. X.; Zhang, Z. Z. Localized Fluorescent Imaging of Multiple Proteins on Individual Extracellular Vesicles Using Rolling Circle Amplification for Cancer Diagnosis. J. Extracell. Vesicles. **2020**, 10, e12025.

(3) Yu, Y. Y.; Zhang, W. S.; Guo, Y. H.; Peng, H. P.; Zhu, M.; Miao, D. D. Engineering of Exosome-Triggered Enzyme-Powered DNA Motors for Highly Sensitive Fluorescence Detection of Tumor-Derived Exosomes. *Biosensors& Bioelectron*. **2020**, *167*, 112482.

(4) Dong, H. L.; Chen, H. F.; Jiang, J. Q.; Zhang, H.; Cai, C. X.; Shen, Q. M. Highly Sensitive Electrochemical Detection of Tumor Exosomes Based on Aptamer Recognition-Induced Multi-DNA Release and Cyclic Enzymatic Amplification. *Anal. Chem.* **2018**, *90*, 4507-4513.

(5) Yin, X. H.; Hou, T.; Huang, B. Z.; Yang, L. M.; Li, F. Aptamer Recognition-Trigged Label-Free Homogeneous Electrochemical Strategy for an Ultrasensitive Cancer-Derived Exosome Assay. *Chem. Commun*. **2019**, *55*, 13705.

(6) Feng, Q. M.; Ma, P. M.; Cao, Q. H.; Yue H.; Guo, Y. H.; Xu, J. J. An Aptamer-Binding DNA Walking Machine for Sensitive Electrochemiluminescence Detection of Tumor Exosomes. *Chem. Commun*. **2020**, *56*, 269.

(7) Huang, L.; Wang, D. B.; Singh, N.; Yang, F.; Gu, N.; Zhang, X. E. A Dual-Signal Amplification Platform for Sensitive Fluorescence Biosensing of Leukemia-Derived Exosomes. *Nanoscale*, **2018**, *10*, 20289.

(8) Zhao, L.; Sun, R. J.; He, P.; Zhang, X. R. Ultrasensitive Detection of Exosomes by Target-Triggered Three-Dmensional DNA Walking Machine and Exonuclease III-

Assisted Electrochemical Ratiometric Biosensing. *Anal. Chem*. **2019**, *91*, 14773-14779.